ARMY RESEARCH LABORATORY

Effect of Precrack "Halos" on K_{Ic} Determined by the Surface Crack in Flexure Method

by Jeffrey J. Swab
and George D. Quinn

ARL-TR-1575

December 1997

The findings in this report are not to be construed as an official Department of the Army position unless so designated by other authorized documents.

Citation of manufacturer's or trade names does not constitute an official endorsement or approval of the use thereof.

Destroy this report when it is no longer needed. Do not return it to the originator.

ERRATA SHEET

re: ARL-TR-1575, "Effect of Precrack 'Halos' on K_{Ic} Determined by the Surface Crack in Flexure Method," by Jeffrey J. Swab and George D. Quinn

Request the following pen-and-ink change be made to Reference 45, Page 24:

That portion of the reference which reads:

Army Nationals and Mechanics Research Center, 1985

should be changed to read:

Army Materials and Mechanics Research Center, 1985.

Army Research Laboratory
Aberdeen Proving Ground, MD 21005-5066

ARL-TR-1575 **December 1997**

Effect of Precrack "Halos" on K_{Ic} Determined by the Surface Crack in Flexure Method

Jeffrey J. Swab
Weapons and Materials Research Directorate, ARL

George D. Quinn
National Institute of Standards and Technology, Ceramics Division

Abstract

The surface crack in flexure (SCF) method, which is used to determine the fracture toughness of dense ceramics, necessitates the measurement of precrack sizes by fractographic examination. Stable crack extension may occur from flaws under ambient, room temperature conditions, even in the relatively short time under load during fast fracture strength or fracture toughness testing. In this paper, fractographic techniques are used to characterize evidence of stable crack extension, a halo, around Knoop indentation surface cracks. Optical examination of the fracture surfaces of a high-purity Al_2O_3, an AlN, a glass-ceramic, and a MgF_2, revealed the presence of a "halo" around the periphery of each precrack. The halo in the AlN was merely an optical effect due to crack reorientation while the halo in the MgF_2 was due to indentation-induced residual stresses initiating crack growth. However, for the Al_2O_3 and the glass-ceramic environmentally-assisted slow crack growth (SCG) was the cause of the halo. In the latter two materials this stable crack extension must be included as part of the critical crack size in order to determine the appropriate fracture toughness.

Acknowledgments

Partial support for this program was furnished by the Propulsion Systems Materials Program of the U.S. Department of Energy, Office of Transportation Technologies, under contract DE-AC05-84OR21400 with Martin Marrietta Energy Systems, Inc. The authors would also like to thank Prof. R. N. Katz of Worcester Polytechnic Institute and Mr. Roy Rice for supplying the AlN and MgF_2 materials, respectively.

Table of Contents

List of Figures

List of Tables

1. Introduction

1.1 Summary of the Surface Crack in Flexure (SCF) Method. The use of indentation-induced flaws to measure the fracture toughness of brittle monolithic ceramics has been employed since the early 1970s when Kenny [1] first used Knoop-indentation-induced precracks to measure the fracture toughness (K_{Ic}) of cemented tungsten carbides. The technique he employed was very simple: introduce a precrack by indenting one surface of a rectangular beam specimen with a row of Knoop indentations oriented normal to the specimen long axis, fracture the specimen in flexure with the indented surface in tension, and calculate the toughness using the precrack size and fracture stress.

Over the next several years, Petrovic and his associates [2–8] developed and refined the technique as an alternative to classic fracture mechanics tests (double torsion and double cantilever beam), which use large cracks popped in from a saw-cut. Vickers and Knoop indentations were both used to introduce precracks, but the Knoop indentation became the preferred method due to the simple crack pattern that it generates. During this period, they realized that the residual stresses that accompany the indentation have a pronounced effect on the resultant fracture toughness value. These residual stresses combine with the applied stress to produce a lower fracture strength, resulting in lower a K_{Ic} value. Elimination of the residual stresses through material removal or annealing yielded toughness values comparable to those generated with double torsion methods [4–5]. Material removal is the preferred method of eliminating the residual stresses since annealing can lead to flaw healing or blunting [3] and may, in some materials, lead to undesirable microstructural changes.

Recent efforts by Quinn and colleagues [9–14] have further refined the method. They conducted an international round-robin exercise [9], involving 20 agencies, to examine the precision of the SCF method and its standardization potential. They also applied the method to over 40 materials, ranging from low-toughness glasses to high-toughness zirconias. These refinements have lead to the

inclusion of the method as one of three techniques in a new fracture toughness provisional standard (PS)* recently adopted by the American Society for Testing and Materials (ASTM).†

The SCF method requires the Knoop indentation of a specimen, removal of the residual stresses via grinding and/or polishing, fracture of the specimen in flexure, fractographic examination and determination of the precrack size, and calculation of the toughness according to equation (1) for a semicircular or semielliptical surface crack in tension or flexure:

$$K_{Ic} = Y \sigma \sqrt{a}, \tag{1}$$

where

Y is the stress intensity shape factor (dimensionless),
σ is the flexure strength of the specimen (MPa), and
a is the crack depth (m).

Two of the benefits of this method are the small precrack size, which is on the order of the size of natural flaws observed in ceramics, and the ability to control this size through the indentation load. The major liability is the need to measure the precrack, which, in some materials, can be difficult. SCF fractographic techniques are described in detail in Quinn, Gettings, and Kübler [12].

1.2 Precrack Halos. "Halos" (rings that are darker or brighter than the precrack) have been seen around precracks in a variety of ceramic materials [4–6, 10–23]. In many of these cases [4–6, 15, 16, 18–20], the appearance of a halo is the result of slow crack growth (SCG) during elevated temperature testing. These halos are part of a sequential set of fracture surface markings that emanate from a strength-limiting flaw when a ceramic is fractured in tension [24–26]. The features result from an increase in the crack velocity as the crack propagates through the body. Associated

* American Society for Testing and Materials. "Standard Test Methods for the Determination of Fracture Toughness of Advanced Ceramics at Ambient Temperatures." PS No. 070-1997, 1997.

† American Society for Testing and Materials, 110 Barr Harbor Drive, West Conshohocken, PA 19428.

with the sequential formation of each feature is an increase in the microscopic texture (increased roughness). This change in texture changes the optical reflectivity, enabling the delineation of each feature on the fracture surface. In fact, when measuring the size of such features, it is recommended that an optical microscope be used instead of a scanning electron microscope (SEM) because the former has excellent contrast effects [26].

Alumina [10], silicon nitride [9, 11, 12], glass-ceramic [12], sialon [21], and magnesium fluoride [22, 23] have all been shown to exhibit halos around indentation-induced precracks on the fracture surface after room-temperature tests. Tracy and Quinn [10] reported a halo around the periphery of the precrack when they applied the SCF method to a high-purity fine-grained (1–6 μm) Al_2O_3 (Figure 1). (The halo appears as a dark ring around the precrack under optical examination.) They also reported evidence of stable crack extension on the fracture surface, corresponding to the halo. The halo was most pronounced in specimens that had been precracked at indentation loads of 29.4 and 49 N. Additional indentation loads of 69, 113, 167, and 255 N were used in this study. The relative size of the halo diminished as the indentation load and, thus, the precrack size increased. The halo *was not* included as part of the critical crack size used in their toughness calculations [10]. Their plot of apparent toughness vs. initial precrack size (Figure 2) suggested a possible R-curve behavior for this material.

There are several possible explanations for the appearance of halos on the fracture surface around Knoop-indentation-induced precracks, as discussed in sections 1.2.1–1.2.4.

1.2.1 Environmentally Assisted Slow Crack Growth. Testing at elevated temperatures can result in slow crack growth. As previously mentioned, SCG growth at elevated temperatures can lead to stable crack extension, but at room temperature, environmentally assisted SCG can also be active due to moisture present under ambient laboratory conditions. This could occur prior to the removal of the residual stresses associated with the indentation or during the 15–30 s it typically takes to conduct a flexure test.

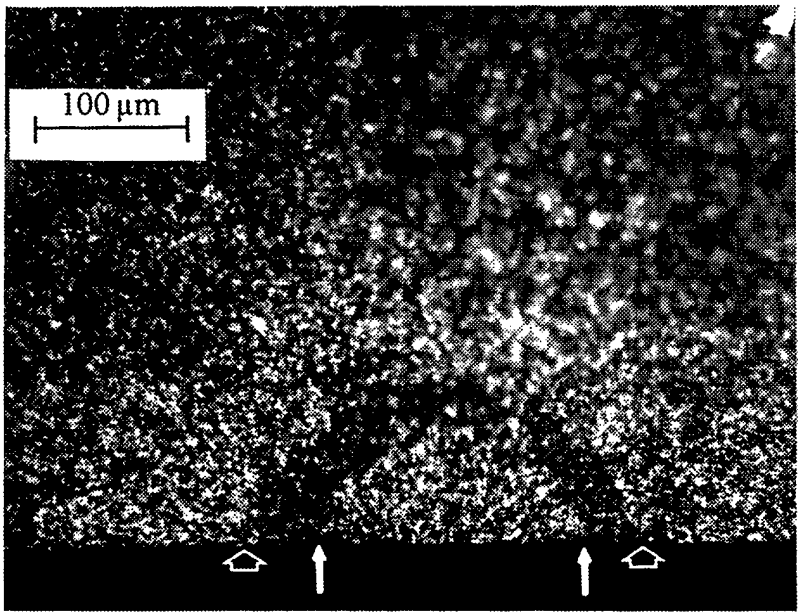

Figure 1. Optical Photograph of a Knoop-Indentation-Induced Precrack (29.4 N Load) and Associated Halo in AD-999. Solid Arrows Outline Precrack, and Open Arrows the Halo.

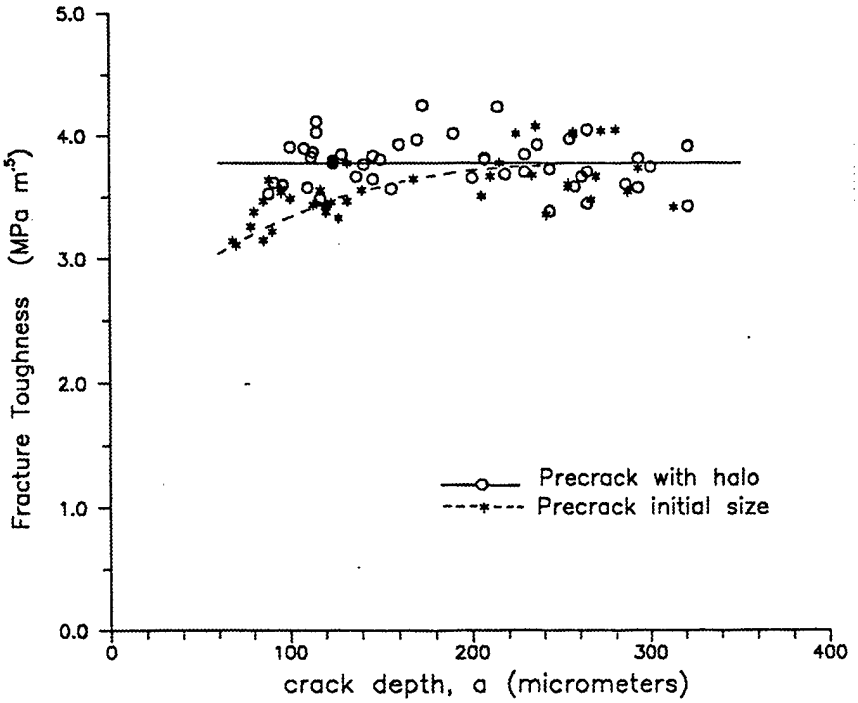

Figure 2. Plot of Apparent Toughness vs. Precrack Depth for AD-999. The Stars Include All of the Data From Tracy and Quinn [10] and the Seven Specimens From the Present Study Without Incorporation of the Halo. The Circles Correspond to the Same Data, but With the Halo Included.

1.2.2 Crack Reorientation. It is well known that cracks aligned out of the plane of an applied tensile stress field will realign normal to the maximum tensile stress field during failure [27]. In the round-robin exercise, Quinn, Kübler, and Gettings [9] had the participants intentionally misalign the specimens with a slight tilt of 1/2° during precracking. This enhanced the detectability of the precrack for fractography, but forced the precrack to enter the specimen at an angle of 1/2° to 5°. This realignment may be enough to account for a halo since, under optical viewing, each region could appear different due to variations in reflectivity created by the arrangement of the different planes.

1.2.3 R-Curve Behavior. Some ceramic materials exhibit R-Curve behavior [28–35] (rising fracture toughness with an increase in crack size). This behavior is most pronounced when small (on the order of naturally occurring flaws) precracks are used. In transformation-toughened zirconia [28–31], extension of a small crack of as little as 10 μm has been shown to produce a 3–5 fold increase in fracture toughness [31].

1.2.4 Stable Crack Extension From Indentation-Induced Residual Stresses. Although the SCF method stipulates that residual stresses must be removed prior to fracture testing, these stresses are acting on the precrack for a time and may, in certain materials, lead to stable crack extension. There are several examples in the literature where residual stresses may have contributed to the formation of a halo. Govila [16] and Quinn, Gettings, and Kübler [12] conducted studies on Si_3N_4 and a glass-ceramic, respectively, in which the residual stresses were not removed. They presented optical photographs showing a halo around the precrack. Marshall [27] showed that, under mixed-mode loading, Knoop-indentation cracks that had the residual stresses, still present extended and aligned normal to the maximum tensile stress before failure. Indentation cracks that had the residual stresses removed through annealing did not undergo any stable crack extension, but propagated unstably and with an abrupt change in fracture plane.

Since measurement of the precrack is an important step in the SCF method, it is important to elucidate the cause of the halo and its effect on the apparent fracture toughness. In this report, we investigate halos that appear around SCF precracks in a variety of ceramics tested at room temperature.

2. Experimental Procedure

All of the materials investigated were fine-grained fully dense materials that have been well characterized.* Information on each material is listed in Table 1.

Table 1. Materials Investigated

Material	Manufacturer	Processing	Density (g/cm^3)	Indentation Load (N)
Al_2O_3 (AD-999)[a]	Coors Ceramics	Sintered	3.97	29.4
AlN[b]	Dow Chemical	Hot-Pressed (No Sintering Aid)	3.26	49.0
Pyroceram 9603[c]	Corning	Melt, Heat Treat	2.59	49.0
MgF_2	—	Hot-Pressed	3.18	29.4

[a] AD-999 is sintered to full density with minimal glass phase.

[b] The AlN powder is prepared by a carbothermal process and hot-pressed without a sintering aid to full density.

[c] Pyroceram 9603 is a cordiertie glass-ceramic, but has different amounts of secondary phases, such as cristobalite and magnesium titanate, compared to the more common Pyroceram 9606.

Flexure specimens were machined from plates or billets according to the machining guidelines in ASTM C 1161.† The MgF_2 specimens were 3 mm × 4 mm × 25 mm in size, while specimens for the remaining materials were standard 3-mm × 4-mm × 50-mm flexure bars. In addition to the normal machining procedure, one 4-mm-wide face of each bar was finished with a 900-grit wheel. This face was then indented with a Knoop indenter (see Table 1 for the indentation load used for each material) to create a precracked specimen. During indentation, the specimen was tilted ≈1/2°

* Certain commercial materials or equipment are identified in this report to adequately specify the experimental procedure. Such identification does not imply endorsement by the U.S. Army Research Laboratory (ARL) or the National Institute of Standards and Technology (NIST) nor does it imply that these materials or equipment are necessarily the best for the purpose.

† American Society for Testing and Materials. "Standard Test Method for Flexural Strength of Advanced Ceramics at Ambient Temperature." ASTM C 1161, *1997 Annual Book of ASTM Standards*, vol. 15.01, 1997.

off perpendicular to the diamond indenter axis. This tilt introduced the precrack at a slight angle that proved beneficial to precrack detection during subsequent fractographic analysis.

Once the specimen was precracked, the long diagonal of the Knoop impression was measured to determine the indentation depth and identify the amount of material to be removed. The amount of material removed was nominally 4.5 h, where h is the indentation depth. Details on the material removal process and why this specific amount of material is removed can be found in Quinn, Kübler, and Gettings [9]; Tracy and Quinn [10]; Gettings and Quinn [11]; and Quinn, Gettings, and Kübler [12].

Flexure strength was determined using a standard 20-mm × 40-mm fully articulating four-point fixture at a cross head speed of 0.5 mm/min in accordance with ASTM C 1161. The smaller MgF_2 specimens were tested at the same crosshead speed, but on a semi-articulating four-point fixture with inner and outer spans of 10 and 20 mm, respectively. At this loading rate, failure times were 15–30 s, during which the material could be susceptible to slow crack growth. Testing was conducted under ambient laboratory conditions (temperature: 20–25° C; relative humidity: 35–50%) and at room temperature in a flowing, ultrahigh purity, dry nitrogen environment. In the latter case, once a preload was applied to the specimen, a plastic sleeve was placed around the test setup, and a nitrogen flow of ≈7 ml/min was started. Five minutes was allowed to elapse to purge the system. The fast fracture test was then conducted with the nitrogen still flowing.

After fracture, both mating halves of the fracture surface were fractographically examined to characterize the precrack.* One of the mating halves was optically photographed at ≈200x. A layer of Au (≈5 nm) was sputtered on to the fracture surface of the Al_2O_3, the glass-ceramic, and MgF_2 specimens to enhance reflectivity and ease of optical photography. Many specimens were examined with the SEM for precrack size measurements and possible changes in the fracture morphology associated with the precrack and halo. The depth (a) and width (2c) of each precrack were determined from optical and/or SEM photographs, and the stress intensity shape factor (Y) at the

* American Society for Testing and Materials. "Fractography and Characterization of Fracture Origins in Advanced Ceramics." ASTM C 1322-96a, *1997 Annual Book of ASTM Standards*, vol. 15.01, 1997.

precrack depth and the precrack boundary at the specimen surface were calculated for each specimen from the empirical equations of Newman and Raju [36]. The maximum Y value was then used to compute the apparent fracture toughness (K_{Ic}) according to equation (1).

3. Results and Discussion

3.1 Alumina (Al_2O_3). All 39 specimens previously tested by Tracy and Quinn [10] were optically reexamined to ascertain the size of the halo and its effect on the apparent fracture toughness (Table 2). An optical examination was sufficient since their work [10] showed that there was excellent agreement between the precrack sizes determined from SEM and optical photographs. The small differences between the optical and SEM analysis typically resulted in a $\leq$0.1-MPa$\sqrt{m}$ change in the calculated toughness.

Table 2. Average SCF Fracture Toughness Values for AD-999 Alumina

Load (N)	No. of Specimens	K_{Ic} Without Halo (MPa$\sqrt{m}$)	K_{Ic} With Halo (MPa$\sqrt{m}$)
29.4	7	3.41 ± 0.22	3.88 ± 0.17
29.4	3	3.26 ± 0.08[a]	3.58 ± 0.05
49.0	5	3.34 ± 0.10[a]	4.00 ± 0.16
68.9	9	3.47 ± 0.14[a]	3.72 ± 0.13
112.7	9	3.49 ± 0.18[a]	3.69 ± 0.14
166.7	9	3.52 ± 0.15[a]	3.66 ± 0.16
254.9	4	3.80 ± 0.11[a]	4.05 ± 0.13
Nat. Flaws	7	2.4 - 3.5	No Halos

[a] Specimens from Tracy and Quinn [10]. Uncertainty levels listed are ±1 standard deviation.

Halos were also observed around the precracks in seven additional Al_2O_3 specimens, precracked at 29.4 N, and tested in the present study. The average fracture toughness of these seven specimens,

without the halo, was 3.41 ± 0.14 MPa$\sqrt{m}$, which is in excellent agreement with the value reported earlier by Tracy and Quinn [10] (Table 2) for the same indentation precrack load. If the halo is included as part of the critical crack size, the average toughness increases 13% to 3.88 ± 0.17 MPa$\sqrt{m}$.

Figure 2 shows the data for the 39 specimens tested by Tracy and Quinn [10], as well as the data for the seven specimens tested in the present study. In general, for each datum, the incorporation of the halo into the critical crack size shifts the datum upward (higher toughness) and to the right (larger crack depth). The effect is most pronounced for the smaller precracks.

As the indentation load increases, the relative size of the halo decreases. At the highest loads, the halo did not appear to uniformly ring the entire precrack. It was negligible at the deepest point, but grew wider as it approached the specimen tensile surface (Figure 3). Incorporation of the halo into the critical crack size eliminated the suggested R-curve behavior (Figure 2) and provided fracture toughness values which are comparable with values generated using large-crack fracture toughness techniques, see Table 3.

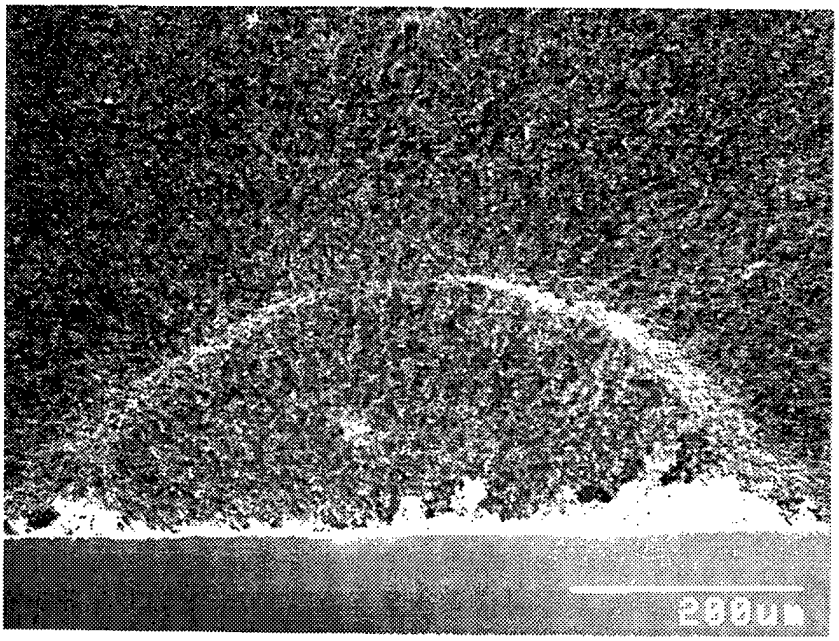

Figure 3. SEM Photograph of a Knoop Indentation-Induced Precrack (254.9 N Load). Note There Is No Halo Evident at the Deepest Portion of the Precrack.

Table 3. Long Crack Fracture Toughness Values for AD-999 Alumina

Reference	K_{Ic} (MPa$\sqrt{m}$)[a]	Test Technique
Tracy and Quinn [10]	4.12 ± 0.25 (4)	Double Torsion
Swanson [37]	4.44	Double Cantilever Beam
Simpson [38]	3.99	Double Cantilever Beam
Antis et al. [39]	3.92	Single-Edge Notched Beam
Barker [40]	3.9	Double Cantilever Beam

[a] The number in parenthesis indicates the number of specimens. Uncertainty levels listed are ±1 standard deviation.

A detailed SEM fractographic analysis of a precrack with a halo (Figure 4a) revealed differences in the fracture morphology in the precrack region, halo region, and fast fracture region (Figures 4b–d). The dominant fracture mechanism in the precrack region was transgranular fracture (Figure 4b) while the halo region had a mixture of transgranular and intergranular fracture (Figure 4c). Outside the halo, in the fast fracture region, transgranular fracture was again the dominant failure mechanism (Figure 4d). The increase in intergranular fracture within the halo region suggests that environmentally assisted SCG had occurred at room temperature, probably during the fracture test. High purity (≥99%) aluminas have been shown to exhibit SCG at room temperature [41–44] and SCG exponents (n) of approximately 20–40 having been reported [41–45]. Ferber and Brown [42] noted that the SCG was the greatest in the presence of water.

Additional specimens of the same alumina, from an extensive round-robin exercise [46], were examined to estimate the fracture toughness from the naturally occurring flaws and to determine if a halo was present around these flaws. All of these specimens were tested in lab-ambient conditions. Only seven specimens were amenable to accurate measurement of the strength-limiting flaw size and shape. The resultant fracture toughness ranged from 2.4 to 3.5 MPa$\sqrt{m}$. Halos were not observed around any of these flaws. The strength-limiting flaws in this material are porosity related (pores

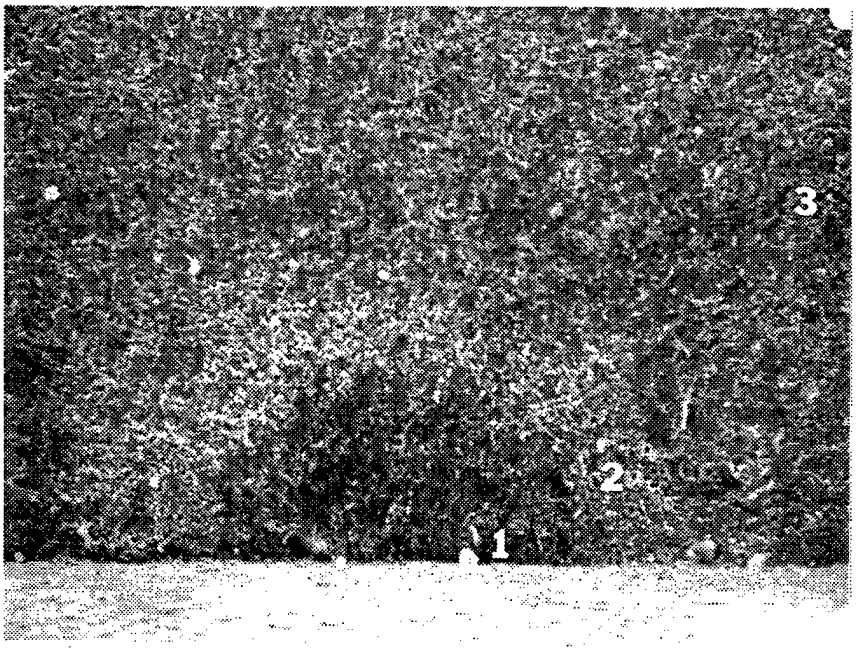

(a) The Precrack and Halo Created in AD-999 With a 29.4 N Load.

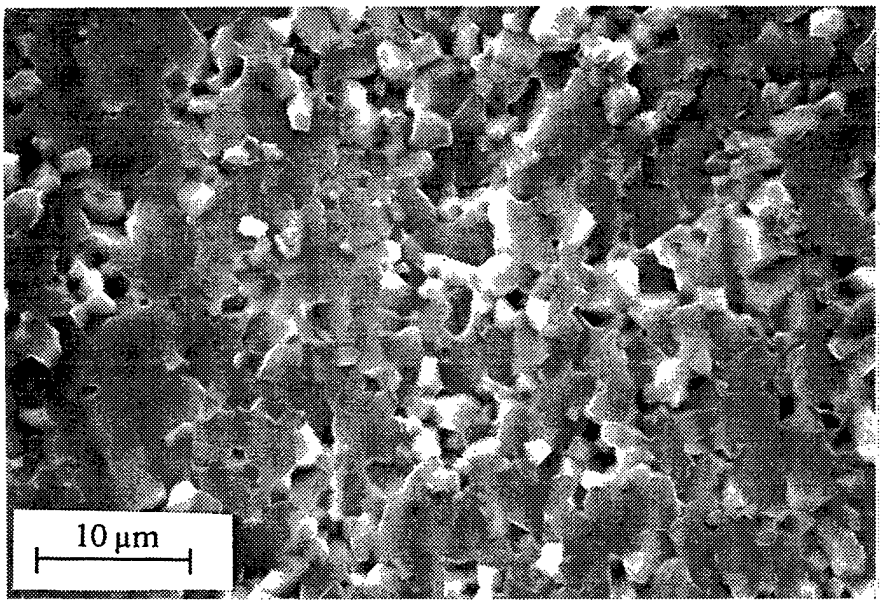

(b) Transgranular Fracture in the Precrack Region - Region 1.

Figure 4. SEM Photographs of AD-999.

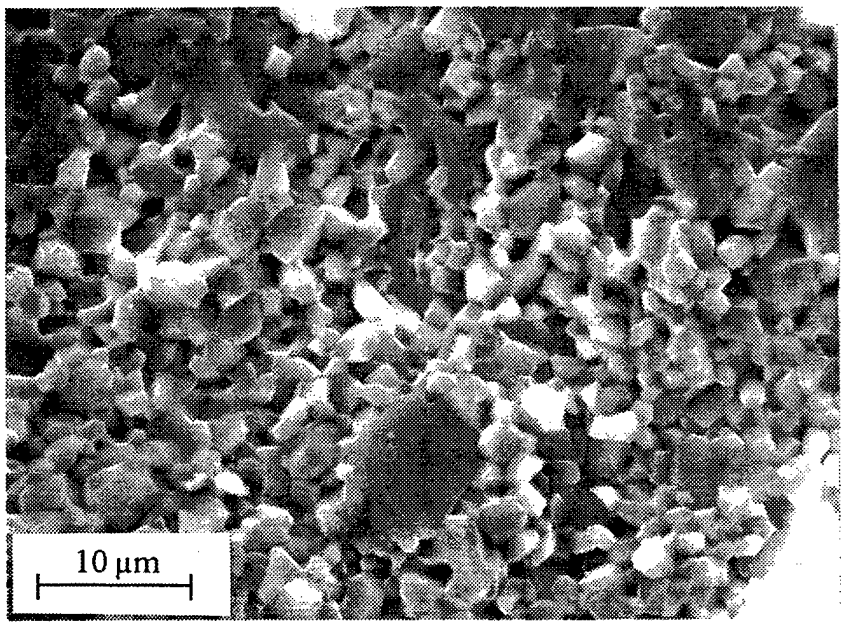

(c) Mixed Transgranular and Intergranular Fracture in the Halo Region - Region 2.

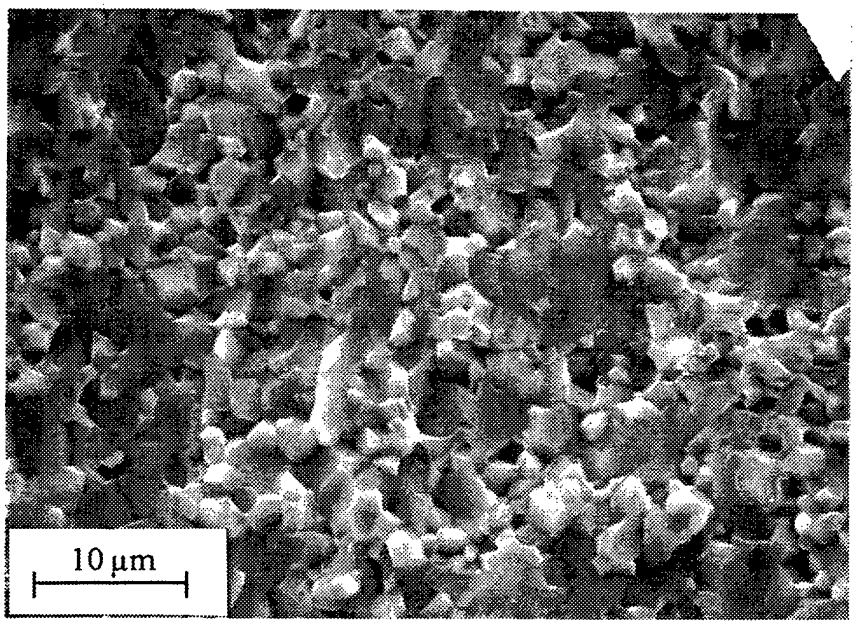

(d) Transgranular Fracture in the Fast Fracture Region - Region 3.

Figure 4. SEM Photographs of AD-999 (continued).

or porous regions), which tend to have a complex geometry that does not allow for accurate measurement of the flaw size or the delineation of a halo, if one exists.

Four additional alumina specimens were precracked under identical conditions using a load of 29.4 N, but flexure testing was conducted in a flowing N_2 environment. No halos were seen in either the optical or SEM photographs of the fracture surfaces of any of these specimen, and there was no difference in fracture morphology on the fracture surface. The resultant fracture toughness value (3.79 ± 0.30 MPa$\sqrt{m}$) agreed with the value (3.88 ± 0.17 MPa$\sqrt{m}$) calculated for the 29.4 N specimens fractured in air when the halo was incorporated into the critical crack size. The difference in the critical crack size was offset by the fracture stress, which was about 10% higher for the specimens tested in flowing N_2. These results clearly indicate that, under ambient laboratory conditions, environmentally assisted SCG can occur in this sintered fine-grained alumina, and it should be taken in to account when computing the fracture toughness. We concluded that the fracture toughness of this sintered alumina is 3.78 ± 0.20 MPa$\sqrt{m}$ (based on 46 specimens) as measured by the surface crack in flexure technique and that the earlier reports [10, 11] of a dependency of K_{Ic} on crack length are incorrect. This should not be surprising since this was a fine-grained equiaxed material, and bridging or crack deflection mechanisms are not significant.

3.2 Aluminum Nitride (AlN). This material also exhibited a halo around the periphery of the precrack during optical examination (Figure 5). Contrary to our previous preliminary report [14], the halo was also evident when viewed with the SEM (it appeared as a white ring in this viewing mode, as opposed to a black ring in optical analysis), and there was a difference in fracture morphology. The change in morphology was only between the halo and the fast fracture region. The halo and precrack exhibited approximately an even mix of transgranular and intergranular fracture, while the fast fracture region was predominantly (>90%) transgranular. Katz et al. [47] reported a similar mix of transgranular and intergranular fracture in the mirror, mist, and hackle regions around naturally occurring flaws in tensile specimens of the identical material. The fracture mode in AlN depends upon the amount of boundary phase and the morphology of the AlN (which can be equiaxied or plate-like). The AlN examined in this study had low oxygen content ($\approx$1 weight-percent) and equiaxed grains. No SCG is expected in this material since it has no intended

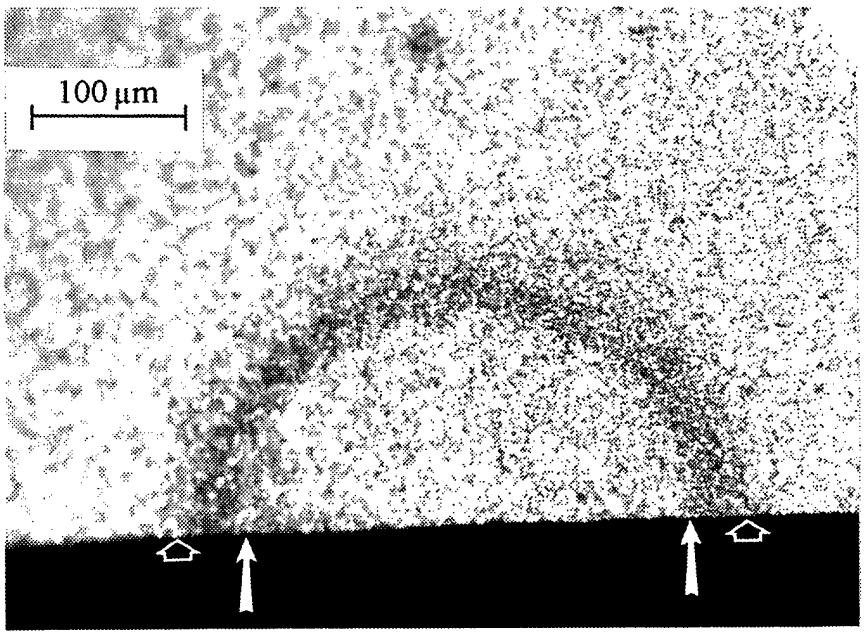

Figure 5. Optical Photograph of a Knoop Indentation-Induced Precrack (49.0 N Load) and the Associated Halo in AlN. The Halo Is Due to Crack Reorientation During Fracture.

sintering aid and a very low oxygen content [48]. Studies on AlN have shown that room [49] and elevated temperature flexure strength [50], as well as room-temperature static fatigue resistance [51], are all a function of the oxygen content.

Sakai [49, 50] noted that an increase in oxygen content above approximately 2.7 weight-percent results in a decrease in flexure strength, and the fracture mode at room temperature was a function of oxygen content [49]. Intergranular fracture was common for oxygen contents between 1.1 and 2.7 weight-percent, while, above this level, fracture was predominantly transgranular. The change was attributed to the plate-like structure of the AlN polytypes that form in hot-pressed AlN containing more than 2.7-weight-percent oxygen. Porosity may also contribute to the differences in fracture morphology reported in the this study and by Sakai [49, 50]. The AlN Sakai [49, 50] tested tended to be around 98% dense, while in the present study, the material was fully dense. O'Day and Leatherman [51] found that the room-temperature static fatigue resistance of AlN

sintered with various amounts of Y_2O_3 was minimal, except when there was a large amount (13 volume-percent) of an oxygen-rich second phase present.

The calculated toughness values, without including the halo size, are comparable to other toughness values reported in the literature [47, 48, 52] (Table 4) for the identical material. Inclusion of the halo in the critical crack size of the AlN results in a toughness value significantly higher than any of the values listed in Table 4. These facts indicate that the halo may merely be an optical effect created by the reorientation of the crack to the plane of maximum tensile stress.

Table 4. Fracture Toughness Values for the Hot-Pressed AlN Examined in This Study

Reference	K_{Ic} (MPa$\sqrt{m}$)	Test Technique
Present Study	2.66 ± 0.11 (6)[a]	Surface Crack in Flexure in Air
Present Study	2.74 ± 0.04 (6)	Surface Crack in Flexure in N_2
Katz et al. [47]	2.53 ± 0.35 (7)	Estimated From Natural Flaws
Skeele, Slavin, and Katz [48]	2.70 ± 0.24 (5)	Chevron Notch, Short Bar
Katz et al. [52]	2.62 ± 0.15 (21)	Single Edge Precracked Beam

[a] The Number in parenthesis indicates number of specimens. Uncertainty levels listed are ±1 standard deviation.

To determine if the halo truly was an optical effect, an additional set of SCF tests was conducted, but flexure testing was done in a flowing dry N_2 environment. Due to the limited amount of material available, the specimens used were the fractured halves from the lab-ambient test set. The resulting specimens were nominally 2.8 mm × 4 mm × 25 mm. The flexure test configuration and test parameters were the same as for the MgF_2 material.

Halos were also observed around these precracks, but they were not as distinct, and there was essentially no change in fracture morphology between the regions. The apparent fracture toughness is 2.74 ± 0.04 MPa$\sqrt{m}$, which is in excellent agreement with the toughness from the lab-ambient tests. Incorporation of the halo again resulted in a higher apparent toughness. We believe that the

toughness of this material is 2.70 ± 0.09 MPa$\sqrt{m}$ (based on 12 specimens), and the halo is present due to crack reorientation during initial crack extension at criticality. As noted in section 2, these precracks were intentionally tilted to enhance fractographic detectability.

3.3 Pyroceram 9603. A halo was not observed around any of the precracks during optical examination of specimens that had been tested in lab-ambient conditions. However, a halo could be seen when an SEM stereo pair of photographs was viewed in a stereo viewer. Inclusion of the halo in the critical crack size yielded an average toughness (for 5 specimens) of 2.30 ± 0.10 MPa$\sqrt{m}$. This is in excellent agreement with the 2.4 ± 0.1 MPa$\sqrt{m}$ obtained by constant moment double cantilever beam tests [53]. (Without the halo, using only the initial precrack size, the apparent toughness is 1.97 ± 0.11 MPa$\sqrt{m}$, which is too low for this material.) An analysis of the precrack, halo, and fast fracture regions showed no discernible difference in the fracture morphology between the three regions. However, previous work [54, 55] on a similar glass-ceramic (Pyroceram 9606) indicates a susceptibility to environmentally assisted SCG. SCG exponent (n) values of 40 to 100 have been reported in these studies. An additional set of tests was conducted with the exception that fracture occurred in flowing nitrogen. No halos were observed in either optical, SEM, or stereo SEM analysis around the precrack in any of these specimens. The average fracture toughness for four specimens was 2.22 ± 0.22 MPa$\sqrt{m}$, which is in excellent agreement with the previously mentioned data when the halo is included.

This material is susceptible to environmentally assisted SCG, and, similar to the findings reported here for alumina, this growth must be taken in to account when calculating fracture toughness values. However, unlike the alumina, this growth is not easily seen on the fracture surface by optical microscopy. It is recommended that this material be tested in an inert environment to eliminate SCG and avoid the complications created by the halo.

3.4 Magnesium Fluoride (MgF_2). Seven specimens were available for the evaluation of this infrared dome material. All were indented with a 29.4-N Knoop indenter, and a drop of silicone oil was added immediately after the indenter was removed to retard SCG. Five of the seven specimens had the customary 4.5 h of material removed to eliminate the residual stress, while the remaining two

specimens had no material removed.* All flexure testing was conducted in flowing dry N_2 to retard SCG.

The apparent fracture toughness of four specimens (one of the five broke during fast fracture preloading) with the requisite material removed was 0.98 ± 0.04 MPa$\sqrt{m}$, which is in excellent agreement with the value of 0.92 MPa$\sqrt{m}$ reported by Mecholsky [22]. Flexure tests on the two specimens that had the residual stresses intact produced a lower apparent K_{Ic} (0.76 ± 0.05 MPa$\sqrt{m}$), confirming the earlier finding of Wills, Mendiratta, and Petrovic [4] and Petrovic et al. [5] of the impact of residual stresses on K_{Ic}.

Optical fractography revealed no evidence of a halo on three of the four specimens with 4.5 h of material removed. However, the fourth specimen and those specimens that had no material removed exhibited a uniform halo of 20–30 μm around the precrack periphery (Figure 6). In all three of these specimens inclusion of the halo in the critical crack size increased the apparent toughness by 5–6%. Detailed SEM analysis of the various regions on the fracture surface (Figure 7) shows the transition from the intergranular fracture in the halo region to transgranular fracture in the fast fracture region. This is consistent with delayed failure studies [22–23].

It is clear from these tests that the halo in this material is related to the indentation residual stresses. But why did a halo form on the one specimen with material removed? There are several potential explanations: the silicone oil may not have been added quickly enough after indentation to retard SCG, stresses from the material removal step caused the extension, or the preload applied prior to fast fracture testing might have been high enough to initiate growth (the preload applied to this specimen was similar to the preload applied to the specimen that fractured during its application, 18 N). Since specimen preparation and testing were essentially the same for all the specimens, a combination of these factors may account for the halo.

* Testing with no material removed is done to determine the full precrack size after indentation.

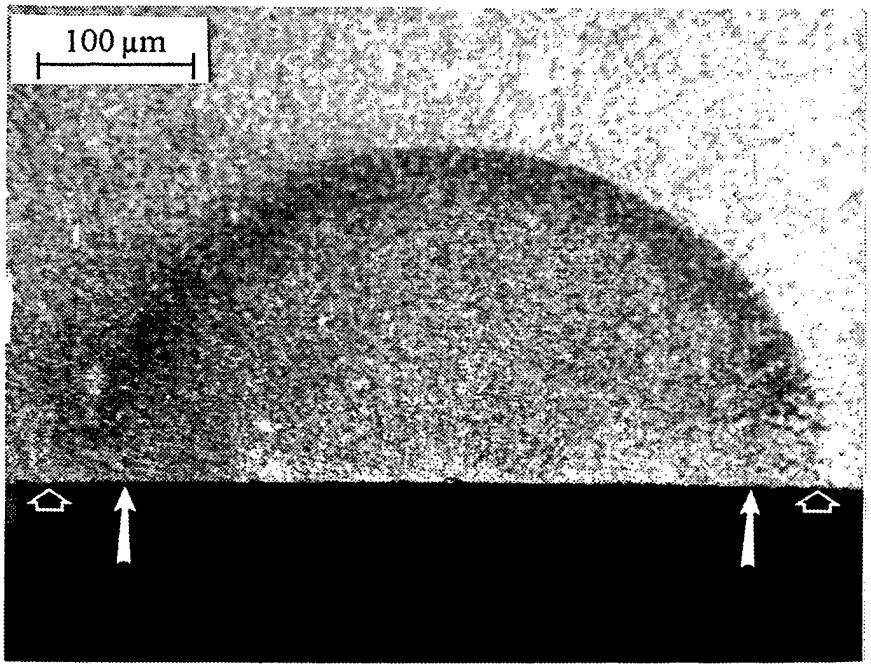

Figure 6. Optical Photograph of a Knoop-Indentation-Induced Precrack (29.4 N Load) and the Associated Halo in MgF_2. The Halo Is Due to the Indentation-Induced Residual Stressed, Even Though the Indent and Residual Stresses Have Been Removed.

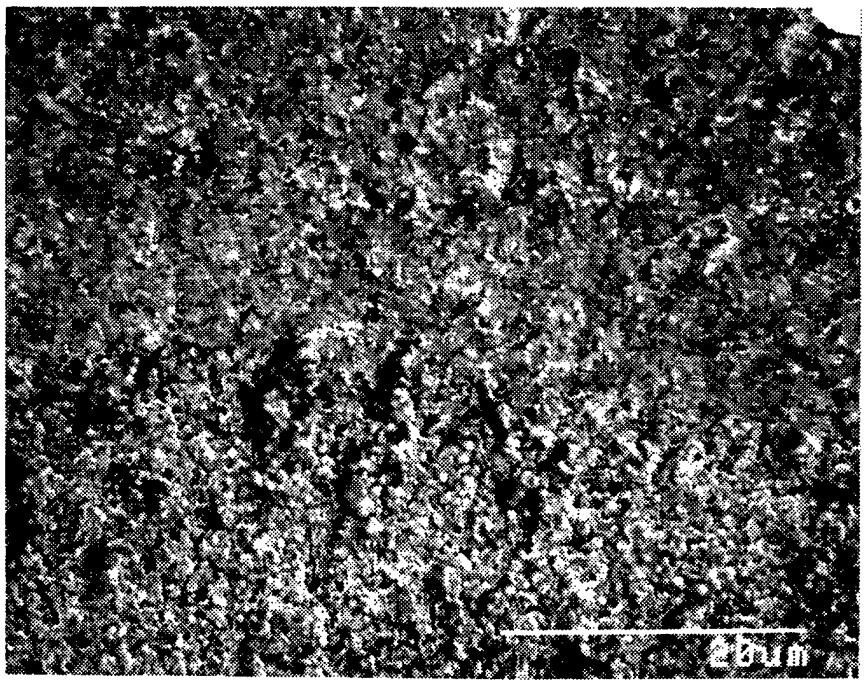

Figure 7. SEM Photograph of the Fracture Surface of an MgF_2 Specimen That Exhibited SCG. The Transition From Intragranular Fracture in the Halo Region to Transgranular Fracture in the Fast Fracture Region Is Clearly Seen.

4. Conclusions

Halos around flaws may arise from several reasons. Environmentally assisted SCG was the cause of the halos in both alumina and the glass-ceramic. Residual stresses associated with the indentation initiated growth in MgF_2. Crack reorientation accounted for the halo observed in AlN. This study has shown that any halo that appears around the periphery of an indentation-induced precrack should be examined for possible changes in the fracture mode; this must be done to ensure that the correct critical crack size is used in the calculation of a critical fracture toughness value from the SCF method. If detailed fractographic analysis proves inconclusive in ascertaining the cause of the halo, additional SCF tests should be conducted in an inert environment to eliminate halos and the interpretation problems associated with them.

INTENTIONALLY LEFT BLANK.

5. References

1. Kenny, P. "The Application of Fracture Mechanics to Cemented Tungsten Carbides." Powder Metallurgy, vol. 14, no. 27, pp. 22–38, 1971.

2. Petrovic, J. J., L. A. Jacobson, P. K. Talty, and A. K. Vasudevan. "Controlled Surface Flaws in Hot-Pressed Si_3N4." *J. Am. Ceram. Soc.*, vol. 58, nos. 3–4, pp. 113–116, 1975.

3. Petrovic, J. J., and L. A. Jacobson. "Controlled Surface Flaws in Hot-Pressed SiC." *J. Am. Ceram. Soc.*, vol. 59, nos. 1–2, pp. 34–37, 1976.

4. Wills, R. R., M. G. Mendiratta, and J. J. Petrovic. "Controlled Surface-Flaw-Initiated Fracture in Reaction-Bonded Si_3N4." *J. Mat. Sci.*, vol. 11, pp. 1330–1334, 1976.

5. Petrovic, J. J., R. A. Dirks, L. A. Jacobson, and M. G. Mendiratta. "Effects of Residual Stresses on Fracture From Controlled Surface Flaws." *J. Am. Ceram. Soc.*, vol. 59, nos. 3–4, pp. 177–178, 1976.

6. Mendiratta, M. G., and J. J. Petrovic. "Slow Crack Growth from Controlled Surface Flaws in Hot-Pressed Si_3N4." *J. Am. Ceram. Soc.*, vol. 61, nos. 5–6, pp. 226–230, 1978.

7. Petrovic, J. J., and M. G. Mendiratta. "Fracture from Controlled Surface Flaws." *Fracture Mechanics Applied to Brittle Materials*, ASTM STP 678, pp. 83–102, S. W. Freiman (ed.), American Society for Testing and Materials, Philadelphia, PA, 1979.

8. Petrovic, J. J. "Effect of Indenter Geometry on Controlled-Surface-Flaw Fracture Toughness." *J. Am. Ceram. Soc.*, vol. 66, no. 4, pp. 277–283, 1983.

9. Quinn, G. D., J. J. Kübler, and R. J. Gettings. "Fracture Toughness of Advanced Ceramics by the Surface Crack in Flexure (SCF) Method: A VAMAS Round Robin." VAMAS Report 17, June 1994.

10. Tracy, C. A., and G. D. Quinn. "Fracture Toughness by the Surface Crack in Flexure (SCF) Method." *Ceram. Eng. Sci. Proc.*, vol. 15, no. 5, pp. 837–845, 1994.

11. Gettings, R. J., and G. D. Quinn. "Fracture Toughness of Ceramics by the Surface Crack in Flexure (SCF) Method." *Fracture Mechanics of Ceramics*, vol. 11, pp. 203–218, R. C. Bradt, D. Munz, and D. P. H. Hasselman (eds.), Plenum, NY, 1996.

12. Quinn, G. D., R. J. Gettings, and J. J. Kübler. "Fractography and the Surface Crack in Flexure (SCF) Method for Evaluating Fracture Toughness of Ceramics." *Fractography of Glasses and Ceramics III*, J. R. Varner, V. D. Fréchette, and G. D. Quinn (eds.), *Ceramic Transactions*, vol. 64, pp. 107–144, The American Ceramic Society, 1996.

13. Quinn, G. D., J. J. Swab, and M. D. Hill. "Fracture Toughness by the Surface Crack in Flexure (SCF) Method: New Test Results." *Ceram. Eng. Sci. Proc.*, vol. 18, no. 4, pp. 163–172, 1997.

14. Swab, J. J., and G. D. Quinn. "Investigation of "Halos." Associated With Fracture Toughness Precracks." *Ceram. Eng. Sci. Proc.*, vol. 18, no. 4, pp. 173–182, 1997.

15. Kinsman, K. K., R. K. Govila, and P. Beardmore. "The Varied Role of Plasticity in the Fracture of Inductile Ceramics." *Deformation of Ceramic Materials*, R. C. Bradt and R. E. Tressler (eds.), pp. 465–482, Plenum Press, 1975.

16. Govila, R. K. "Indentation-Precracking and Double-Torsion Methods for Measuring Fracture Mechanics Parameters in Hot-Pressed Si_3N_4." *J. Am. Ceram. Soc.*, vol. 63, nos. 5–6, pp. 319–326, 1980.

17. Marshall, D. B. "Controlled Flaws in Ceramics: A Comparison of Knoop and Vickers Indentation." *J. Am. Ceram. Soc.*, vol. 66, no. 2, pp. 127–131, 1983.

18. Quinn G. D., and J. B. Quinn. "Slow Crack Growth in Hot-Pressed Silicon Nitride." *Fracture Mechanics of Ceramics*, vol. 6, pp. 603–636, R. C. Bradt, A. G. Evans, D. P. H. Hasselman, and F. F. Lange (eds.), Plenum, NY, 1983.

19. Micski, A., and B. Bergman. "High Temperature Strength of Silicon Nitride HIP-ed With Low Amounts of Yttria or Yttria/Alumina." *J. Eur. Ceram. Soc.*, vol. 6, pp. 291–301, 1990.

20. Quinn, G. D. "Fracture Mechanism Maps for Advanced Structural Ceramics Part 1 Methodology and Hot-Pressed Silicon Nitride Results." *J. Mat. Sci.*, vol. 25, pp. 4361–4376, 1990.

21. Swab, J. J., G. D. Quinn, and M. Bartsch. Unpublished data. National Institute of Standards and Technology, 1996.

22. Mecholsky, J. J. "Intergranular Slow Crack Growth in MgF_2." *J. Am. Ceram. Soc.*, vol. 64 [9], pp. 563–566, 1981.

23. Mecholsky, J. J., and S. W. Freiman. "Fractographic Analysis of Delayed Failure in Ceramics." *Fractography and Materials Science*, ASTM STP 733, eds., L. N. Gilbertson and R. D. Zipp, American Society for Testing and Materials, pp. 246–258, 1981.

24. Fréchette, V. D. "Failure Analysis of Brittle Materials." *Advances in Ceramics*, vol. 28, The American Ceramic Society, 1990.

25. Mecholsky, J. J., Jr., S. W. Freiman, and R. W. Rice. "Fracture Surface Analysis of Ceramics." *J. Mat. Sci.*, vol. 11, pp. 1310–1319, 1976.

26. Mecholsky, J. J., and S. W. Freiman. "Determination of Fracture Mechanics Parameters Through Fractographic Analysis of Ceramics." *Fracture Mechanics Applied to Brittle Materials*, ASTM STP 678, pp. 136–150, S. W. Freiman (ed.), American Society for Testing and Materials, 1979.

27. Marshall, D. B. "Mechanisms of Failure from Surface Flaws in Mixed-Mode Loading." *J. Am. Ceram. Soc.*, vol. 67, no. 2, pp. 110–116, 1984.

28. Marshall, D. B. "Strength Characteristics of Transformation-Toughened Zirconia." *J. Am. Ceram. Soc.*, vol. 69, no. 3, pp. 173–180, 1986.

29. Bennison, S. J., and B. R. Lawn. "Origin Tolerance in Ceramics With Rising Crack Resistance Characteristics." *J. Mat. Sci.*, vol. 24, pp. 3169–3175, 1989.

30. Anderson, R. M., and L. M. Braun. "Technique for the R-Curve Determination of Y-TZP Using Indentation-Produced Flaws." *J. Am. Ceram. Soc.*, vol. 73, no. 10, pp. 3059–3062, 1990.

31. Vicente, A. P., F. Guiberteau, A. Dominguez-Rodriguez, G. W. Dransmann, and R. W. Stienbrech. "Propagation of Short Surface Cracks in Y-TZP." *Euro-Ceramcis II*, vol. 2, pp. 1023–1030, G. Zeigler and H. Hausner (eds.), 1993.

32. White, K. W., and G. P. Kelkar. "Fracture Mechanisms of a Coarse-Grained, Transparent $MgAl_2O_4$ at Elevated Temperatures." *J. Am. Ceram. Soc.*, vol. 75, no. 12, pp. 3440–3444, 1992.

33. Choi, S. R., and J. A. Salem. "Crack-Growth Resistance of *in Situ*-Toughened Silicon Nitride." *J. Am. Ceram. Soc.*, vol. 77, no. 4, pp. 1042–1046, 1994.

34. Xu, H. H. K., C. P. Ostertag, and R. F. Krause, Jr. "Effect of Temperature on Toughness Curves in Alumina." *J. Am. Ceram. Soc.*, vol. 78, no. 1, pp. 260–262, 1995.

35. Stech, M., and J. Rödel. "Method for Measuring Short-Crack R-Curves without Calibration Parameters: Case Studies on Alumina and Alumina/Aluminum Composites." *J. Am. Ceram. Soc.*, vol. 79, no. 2, pp. 291–297, 1996.

36. Newman, J. C., and I. S. Raju. "An Empirical Stress-Intensity Factor Equation for the Surface Crack." *Eng. Fract. Mech.*, vol. 15, nos. 1–2, pp. 185–192, 1981.

37. Swanson, G. D. "Fracture Energies of Ceramics." *J. Am. Ceram. Soc.*, vol. 55, no. 1, pp. 48–49, 1972.

38. Simpson, L. A. "Discrepancy Arising From Measurement of Grain-Size Dependence of Fracture Energy of Al_2O_3." *J. Am. Ceram. Soc.*, vol. 56, no. 11, pp. 610–611, 1973.

39. Antis, G. R., P. Chantikul, B. R. Lawn, and D. B. Marshall. "A Critical Evaluation of Indentation Techniques for Measuring Fracture Toughness: I, Direct Crack Measurements." *J. Am. Ceram. Soc.*, vol. 64, no. 9, pp. 533–538, 1981.

40. Barker, L. M. "Short Rod K_{Ic} Measurements on Al_2O_3." *Fracture Mechanics of Ceramics*, vol. 3, pp. 483–494, R. C. Bradt, D. P. H. Hasselman, and F. F. Lange (eds.), Plenum Press, NY, 1978.

41. Freiman, S. W., K. R. McKinney, and H. L. Smith. "Slow Crack Growth in Polycrystalline Ceramics." *Fracture Mechanics of Ceramics*, vol. 2, pp. 659–676, R. C. Bradt, D. P. H. Hasselman, and F. F. Lange (eds.), Plenum Press, NY, 1972.

42. Ferber, M. K., and S. D. Brown. "Subcritical Crack Growth in Dense Alumina Exposed to Physiological Meida." *J. Am. Ceram. Soc.*, vol. 63, nos. 7–8, pp. 424–429, 1980.

43. Bach, P. W., and B. J. DeSmet. "Subcritical Crack Growth of Wesgo Al-995 Alumina at Room Temperature." ECN-C-92-026, the Netherlands, April 1992.

44. Fett, T., and D. Munz. "Subcritical Crack Growth of Macrocracks in Alumina with R-Curve Behavior." *J. Am. Ceram. Soc.*, vol. 75, no. 4, pp. 958–963, 1992.

45. Quinn, G. D. Unpublished work. Army Nationals and Mechanics Research Center, 1985.

46. Quinn, G. D. "Flexure Strength of Advanced Ceramics-A Round Robin Exercise." *J. Am. Ceram. Soc.*, vol. 73, no. 8, pp. 2374–80, 1990.

47. Katz, R. N., G. Wechsler, H. Toutanji, D. Friel, G. L. Leatherman, T. El-Korchi, and W. Rafaniello. "Room Temperature Tensile Strength of AlN." *Ceram. Eng. Sci. Proc.*, vol. 14, nos. 7–8, pp. 282–91, 1993.

48. Skeele, F. P., M. J. Slavin, and R. N. Katz. "Time-Temperature Dependence of Strength in Aluminum Nitride." *Third International Symposium on Ceramic Materials and Components for Engines*, pp. 710–18, V. J. Tennery (ed.), American Ceramic Society, 1989.

49. Sakai, T. "Effect of Oxygen Composition on Flexural Strength of Hot-Pressed AlN." *J. Am. Ceram. Soc.*, vol. 61, nos. 9–10, pp. 460–461, 1978.

50. Sakai, T. "High-Temperature Strength of AlN Hot-Pressed with Al_2O_3 Additions." *J. Am. Ceram. Soc.*, vol. 64, no. 3, pp. 135–137, 1981.

51. O'Day, M. E., and G. L. Leatherman. "Static Fatigue of Aluminum Nitride Packaging Materials." *Int. J. Microcircuits & Electronic Packaging*, vol. 16, no. 1, pp. 41–48, 1993.

52. Katz, R. N., S. Grendahl, K. Cho, I Bar-on, and W. Rafaniello. "Fracture Toughness of Ceramics in the AlN-SiC System." *Ceram. Eng. Sci. Proc.*, vol. 15, no. 5, pp. 877–84, 1994.

53. Lewis, D. "Observations on the Strength of a Commercial Glass-Ceramic." *Am. Ceram. Soc. Bull.*, vol. 61, no. 11, pp. 1208–1214, 1982.

54. Bansal, G. K., and W. H. Duckworth. "Effects of Moisture-Assisted Slow Crack Growth on Ceramic Strength." *J. Mat. Sci.*, vol. 13, pp. 239–242, 1978.

55. Pletka, B. J., and S. M. Wiederhorn. "A Comparison of Failure Predictions by Strength and Fracture Mechanics Techniques." *J. Mat. Sci.*, vol. 17, pp. 1247–1268, 1982.

INTENTIONALLY LEFT BLANK.

NO. OF COPIES	ORGANIZATION
2	DEFENSE TECHNICAL INFORMATION CENTER DTIC DDA 8725 JOHN J KINGMAN RD STE 0944 FT BELVOIR VA 22060-6218
1	HQDA DAMO FDQ DENNIS SCHMIDT 400 ARMY PENTAGON WASHINGTON DC 20310-0460
1	CECOM SP & TRRSTRL COMMCTN DIV AMSEL RD ST MC M H SOICHER FT MONMOUTH NJ 07703-5203
1	PRIN DPTY FOR TCHNLGY HQ US ARMY MATCOM AMCDCG T M FISETTE 5001 EISENHOWER AVE ALEXANDRIA VA 22333-0001
1	PRIN DPTY FOR ACQUSTN HQS US ARMY MATCOM AMCDCG A D ADAMS 5001 EISENHOWER AVE ALEXANDRIA VA 22333-0001
1	DPTY CG FOR RDE HQS US ARMY MATCOM AMCRD BG BEAUCHAMP 5001 EISENHOWER AVE ALEXANDRIA VA 22333-0001
1	DPTY ASSIST SCY FOR R&T SARD TT T KILLION THE PENTAGON WASHINGTON DC 20310-0103
1	OSD OUSD(A&T)/ODDDR&E(R) J LUPO THE PENTAGON WASHINGTON DC 20301-7100

NO. OF COPIES	ORGANIZATION
1	INST FOR ADVNCD TCHNLGY THE UNIV OF TEXAS AT AUSTIN PO BOX 202797 AUSTIN TX 78720-2797
1	USAASA MOAS AI W PARRON 9325 GUNSTON RD STE N319 FT BELVOIR VA 22060-5582
1	CECOM PM GPS COL S YOUNG FT MONMOUTH NJ 07703
1	GPS JOINT PROG OFC DIR COL J CLAY 2435 VELA WAY STE 1613 LOS ANGELES AFB CA 90245-5500
1	ELECTRONIC SYS DIV DIR CECOM RDEC J NIEMELA FT MONMOUTH NJ 07703
3	DARPA L STOTTS J PENNELLA B KASPAR 3701 N FAIRFAX DR ARLINGTON VA 22203-1714
1	USAF SMC/CED DMA/JPO M ISON 2435 VELA WAY STE 1613 LOS ANGELES AFB CA 90245-5500
1	US MILITARY ACADEMY MATH SCI CTR OF EXCELLENCE DEPT OF MATHEMATICAL SCI MDN A MAJ DON ENGEN THAYER HALL WEST POINT NY 10996-1786
1	DIRECTOR US ARMY RESEARCH LAB AMSRL CS AL TP 2800 POWDER MILL RD ADELPHI MD 20783-1145

NO. OF
COPIES ORGANIZATION

1 DIRECTOR
US ARMY RESEARCH LAB
AMSRL CS AL TA
2800 POWDER MILL RD
ADELPHI MD 20783-1145

3 DIRECTOR
US ARMY RESEARCH LAB
AMSRL CI LL
2800 POWDER MILL RD
ADELPHI MD 20783-1145

ABERDEEN PROVING GROUND

4 DIR USARL
AMSRL CI LP (305)

NO. OF COPIES	ORGANIZATION
10	NATIONAL INSTITUTE OF STANDARDS & TECHNOLOGY GEORGE QUINN BLDG 223 ROOM A329 GAITHERSBURG MD 20899
1	WORCESTER POLYTECHNIC INSTITUTE DR ROBERT KATZ 100 INSTITUTE RD WORCESTER MA 01609
1	ROY RICE 5411 HOPARK DR ALEXANDRIA VA 22310
	ABERDEEN PROVING GROUND
35	DIR USARL AMSRL WM MC MELANIE COLE GARY GILDE DR JERRY LASOLVIA JEFFREY SWAB (30 CPS) AMSRL WM MD KYU CHO AMSRL WM M DR JAMES MCCAULEY

INTENTIONALLY LEFT BLANK.

REPORT DOCUMENTATION PAGE

Form Approved
OMB No. 0704-0188

1. AGENCY USE ONLY *(Leave blank)*	2. REPORT DATE	3. REPORT TYPE AND DATES COVERED
	December 1997	Final, Aug 95 - May 97

4. TITLE AND SUBTITLE

Effect of Precrack "Halos" on K_{Ic} Determined by the Surface Crack in Flexure Method

5. FUNDING NUMBERS

N/A

6. AUTHOR(S)

Jeffrey J. Swab and George D. Quinn

7. PERFORMING ORGANIZATION NAME(S) AND ADDRESS(ES)

U.S. Army Research Laboratory
ATTN: AMSRL-WM-MC
Aberdeen Proving Ground, MD 21005-5066

8. PERFORMING ORGANIZATION REPORT NUMBER

ARL-TR-1575

9. SPONSORING/MONITORING AGENCY NAMES(S) AND ADDRESS(ES)

10.SPONSORING/MONITORING AGENCY REPORT NUMBER

11. SUPPLEMENTARY NOTES

12a. DISTRIBUTION/AVAILABILITY STATEMENT

Approved for public release; distribution is unlimited.

12b. DISTRIBUTION CODE

13. ABSTRACT *(Maximum 200 words)*

The surface crack in flexure (SCF) method, which is used to determine the fracture toughness of dense ceramics, necessitates the measurement of precrack sizes by fractographic examination. Stable crack extension may occur from flaws under ambient room-temperature conditions, even in the relatively short time under load during fast fracture strength or fracture toughness testing. In this paper, fractographic techniques are used to characterize evidence of stable crack extension, a halo, around Knoop indentation surface cracks. Optical examination of the fracture surfaces of a high-purity Al_2O_3, an AlN, a glass-ceramic, and a MgF_2 revealed the presence of a "halo" around the periphery of each precrack. The halo in the AlN was merely an optical effect due to crack reorientation, while the halo in the MgF_2 was due to indentation-induced residual stresses initiating crack growth. However, for the Al_2O_3 and the glass-ceramic, environmentally assisted slow crack growth (SCG) was the cause of the halo. In the latter two materials, this stable crack extension must be included as part of the critical crack size in order to determine the appropriate fracture toughness.

14. SUBJECT TERMS

fracture toughness, fractorgraphy, ceramics, crack growth

15. NUMBER OF PAGES

34

16. PRICE CODE

17. SECURITY CLASSIFICATION OF REPORT	18. SECURITY CLASSIFICATION OF THIS PAGE	19. SECURITY CLASSIFICATION OF ABSTRACT	20. LIMITATION OF ABSTRACT
UNCLASSIFIED	UNCLASSIFIED	UNCLASSIFIED	UL

NSN 7540-01-280-5500

Standard Form 298 (Rev. 2-89)
Prescribed by ANSI Std. 239-18 298-102

USER EVALUATION SHEET/CHANGE OF ADDRESS

This Laboratory undertakes a continuing effort to improve the quality of the reports it publishes. Your comments/answers to the items/questions below will aid us in our efforts.

1. ARL Report Number/Author ARL-TR-1575 (Swab) Date of Report December 1997

2. Date Report Received _____

3. Does this report satisfy a need? (Comment on purpose, related project, or other area of interest for which the report will be used.) _____

4. Specifically, how is the report being used? (Information source, design data, procedure, source of ideas, etc.) _____

5. Has the information in this report led to any quantitative savings as far as man-hours or dollars saved, operating costs avoided, or efficiencies achieved, etc? If so, please elaborate. _____

6. General Comments. What do you think should be changed to improve future reports? (Indicate changes to organization, technical content, format, etc.) _____

CURRENT ADDRESS

_____
Organization

_____
Name E-mail Name

_____
Street or P.O. Box No.

_____
City, State, Zip Code

7. If indicating a Change of Address or Address Correction, please provide the Current or Correct address above and the Old or Incorrect address below.

OLD ADDRESS

_____
Organization

_____
Name

_____
Street or P.O. Box No.

_____
City, State, Zip Code

(Remove this sheet, fold as indicated, tape closed, and mail.)

(DO NOT STAPLE)

DEPARTMENT OF THE ARMY

OFFICIAL BUSINESS

NO POSTAGE
NECESSARY
IF MAILED
IN THE
UNITED STATES

BUSINESS REPLY MAIL
FIRST CLASS PERMIT NO 0001,APG,MD

POSTAGE WILL BE PAID BY ADDRESSEE

DIRECTOR
US ARMY RESEARCH LABORATORY
ATTN AMSRL WM MC
ABERDEEN PROVING GROUND MD 21005-5069